

1 **Probabilistic calibration of a Greenland Ice Sheet model**
2 **using spatially-resolved synthetic observations: toward**
3 **projections of ice mass loss with uncertainties**

4

5 **W. Chang¹, P. J. Applegate², M. Haran¹, K. Keller³**

6 [1]{Department of Statistics, Pennsylvania State University, University Park, PA 16802}

7 [2]{Earth and Environmental Systems Institute, Pennsylvania State University, University
8 Park, PA 16802}

9 [3]{Department of Geosciences, Pennsylvania State University, University Park, PA 16802}

10 Correspondence to: W. Chang (wonchang@psu.edu)

11

12 **Abstract**

13 Computer models of ice sheet behavior are important tools for projecting future sea level rise.
14 The simulated modern ice sheets generated by these models differ markedly as input parameters
15 are varied. To ensure accurate ice sheet mass loss projections, these parameters must be
16 constrained using observational data. Which model parameter combinations make sense, given
17 observations? Our method assigns probabilities to parameter combinations based on how well
18 the model reproduces the Greenland Ice Sheet profile. We improve on the previous state of the
19 art by accounting for spatial information, and by carefully sampling the full range of realistic
20 parameter combinations, using statistically rigorous methods. Specifically, we estimate the
21 joint posterior probability density function of model parameters using Gaussian process-based
22 emulation and calibration. This method is an important step toward calibrated probabilistic
23 projections of ice sheet contributions to sea level rise, in that it uses data-model fusion to learn
24 about parameter values. This information can, in turn, be used to make projections while taking
25 into account various sources of uncertainty, including parametric uncertainty, data-model
26 discrepancy, and spatial correlation in the error structure. We demonstrate the utility of our
27 method using a perfect model experiment, which shows that many different parameter
28 combinations can generate similar modern ice sheet profiles. This result suggests that the large
29 divergence of projections from different ice sheet models is partly due to parametric

1 uncertainty. Moreover, our method enables insight into ice sheet processes represented by
2 parameter interactions in the model.

3

4 **1 Introduction**

5 Accurate projections of future sea level rise are important for present-day adaptation decisions.
6 Global mean sea level has risen 0.2-0.3 m over the last two to three centuries (e.g. Church and
7 White, 2006; Jevrejeva et al., 2008), and this rise is expected to continue in the future (Meehl
8 et al., 2007, Alexander et al., 2013; Edwards 2014a, 2014b). A significant fraction of world
9 population and built infrastructure lies near present-day sea level, and these people and
10 resources are at risk from sea level rise. Projections of sea level rise with sound characterization
11 of the associated uncertainties can inform the design of risk management strategies (e.g.,
12 Lempert et al., 2012).

13 Here, we focus on the Greenland Ice Sheet component of future sea level rise, as estimated by
14 ice sheet models. Computer models of ice sheet behavior make up an important member of a
15 suite of methods for projecting sea level rise. Enhanced mass loss from the Greenland Ice Sheet
16 is just one component of overall sea level rise, which also includes contributions from the
17 Antarctic Ice Sheets, small glaciers, thermal expansion of ocean water, and the transfer of water
18 stored on land to the oceans. However, the Greenland Ice Sheet is a large potential contributor
19 to sea level rise, and also a highly uncertain one; if this ice sheet were to melt completely, sea
20 level would rise by about 7 m (Bamber et al., 2001, 2013; Lemke et al., 2007), and both the rate
21 of ice loss and its final magnitude are uncertain (Lenton et al., 2008). Present estimates of
22 future sea level rise are often derived from semi-empirical extrapolations of tide gauge data
23 (e.g., Rahmstorf, 2007; Grinsted et al., 2009; Jevrejeva et al., 2012) and expert assessments of
24 future ice sheet behavior (e.g., Pfeffer et al., 2008; Bamber and Aspinall, 2013). Ice sheet
25 models complement these methods, in that they provide internally-consistent representations of
26 the processes that are important to the growth and decay of ice sheets. Although imperfect,
27 such models have been the focus of intense development effort since the fourth
28 Intergovernmental Panel on Climate Change assessment report (e.g., Bindschadler et al., 2013;
29 Shannon et al., 2013; Edwards et al., 2014a).

30 To yield accurate projections, ice sheet models must be started from an initial condition that
31 resembles the real ice sheet as closely as possible, both in terms of the spatial distribution and
32 flow of ice and the temperature distribution within the ice body. Ice flow is driven primarily

1 by thickness and surface slope (e.g., Alley et al., 2010), and warm ice deforms more easily than
2 cold ice. Similarly, the melt rate of a patch of the ice sheet's surface is strongly sensitive to its
3 elevation (Born and Nisancioglu, 2012). Thus, errors in the initial condition used for ice sheet
4 model projections will lead to inaccuracies in simulated future ice distributions and sea level
5 rise contributions. In practice, all models include simplifications that also affect projection
6 accuracy (e.g., Kirchner et al., 2011), perhaps more than initial condition errors. However,
7 matching the modern ice sheet is a frequently-recurring theme in the literature (e.g., Ritz et al.,
8 1997; Greve, 1997; Huybrechts, 2002; Stone et al., 2010; Greve et al., 2011; Pollard and
9 DeConto, 2012).

10 The initial condition used in ice sheet models is a function of input parameter values, as well as
11 the spinup method. Because the thermal field within the ice sheet is incompletely known, most
12 modeling studies perform an initialization to bring the simulated ice sheet to a state that is
13 consistent with the present-day climatology (e.g., Stone et al., 2010), climate model output (e.g.,
14 Fyke et al., 2011), or climate history estimated from ice cores (e.g., Applegate et al., 2012).
15 Most studies allow the simulated ice sheet's surface topography to evolve during the spinup
16 period; thus, the estimated initial condition usually does not exactly match the observed ice
17 sheet topography (Bamber et al., 2001, 2013). For example, many studies obtain a simulated
18 modern Greenland ice sheet that is larger than expected (e.g. Heimbach et al., 2008; Stone et
19 al., 2010; Robinson et al., 2010; Vizcaino et al., 2010; Greve et al., 2011; cf. Bamber et al.,
20 2001, 2013). Ice sheet models have many uncertain parameters that affect the softness of the
21 ice, the speed of basal sliding, and the intensity of surface melting, among other processes (Ritz
22 et al., 1997; Hebel et al., 2008; Stone et al., 2010; Fitzgerald et al., 2011; Applegate et al.,
23 2012). Adjusting these parameters changes the simulated modern ice sheet (Stone et al., 2010;
24 Applegate et al., 2012).

25 Despite the importance of achieving a good match between ice sheet model output and the
26 present-day ice geometry, it remains unclear how to use data on the modern ice sheet to assess
27 the relative plausibility of different model runs, in cases where the modeled ice sheet surface
28 topography can evolve freely. The root-mean-squared error (RMSE) is sometimes used for this
29 purpose (e.g., Greve and Otsu, 2007; Stone et al., 2010). However, it is unclear how to translate
30 the RMSE values from a set of model runs into probabilistic projections of ice volume change,
31 as required for sea level studies. Using a probability model that accounts for various
32 uncertainties, as we do here, helps overcome this limitation. Recent work by McNeall et al.

1 (2013) and Gladstone et al. (2012) partly addresses the challenge of identifying appropriate
2 parameter combinations, given observations and a freely-evolving ice sheet model. McNeall
3 et al. (2013) train a statistical emulator (e.g., Sacks et al., 1989; Kennedy and O'Hagan, 2001)
4 to relate input parameter combinations to highly-aggregated metrics describing the Greenland
5 ice sheet's geometry (volume, area, and maximum thickness; Ritz et al., 1997; Stone et al.,
6 2010), using a previously-published ensemble of ice sheet model runs (Stone et al., 2010). The
7 work of McNeall et al. (2013) is groundbreaking in its application of a computationally-efficient
8 statistical emulator to an ice sheet model, allowing estimation of model output at many more
9 design points than would have been possible with the model itself. However, the highly-
10 aggregated metrics used by McNeall et al. (2013) neglect information on the spatial distribution
11 of ice, which might further limit the parameter combinations that agree well with the observed
12 geometry of the modern ice sheet. Moreover, their calibration approach is based on "historical
13 mapping" and does not provide probabilistic projections. Gladstone et al. (2012) proposed a
14 simple, but statistically robust, probabilistic approach for calibrating a flowline model of Pine
15 Island Glacier in West Antarctica, but their approach is applicable only when the ice flow model
16 is computationally cheap and the observational data include only a small number of
17 observations.

18 A second challenge involves characterizing the effects of input parameter choice on the
19 agreement between modeled and observed ice sheets. In an ensemble of Greenland Ice Sheet
20 model runs carried out by Applegate et al. (2012; described below), the parameter combinations
21 that agree well with the modern ice sheet's volume are widely distributed over parameter space,
22 with no easily-discernable structure. This result may arise from uncharacterized interactions
23 among the model parameters. This outcome also has strong implications for model projections
24 of sea level rise from the ice sheet, in that the model runs that agree well with the modern
25 volume constraint give widely diverging sea level rise projections (Applegate et al., 2012).

26 Finally, estimates of future sea level rise require projections of ice volume change with well-
27 characterized uncertainties. Perturbed-parameter ensembles (e.g., Stone et al., 2010; Applegate
28 et al., 2012, Edwards et al., 2014a) represent an important step toward this goal, but the
29 relatively small number of model runs that can be performed in a reasonable time (usually 10^2 -
30 10^3 ; Stone et al., 2010; Applegate et al., 2012) are insufficient to fully explore model parameter
31 space. As McNeall et al. (2013) demonstrate, statistical emulators help overcome this
32 dimensionality problem; however, some method for assigning plausibility scores to the

1 emulator output is also needed. In a slightly different but relevant context, Little et al. (2013)
2 and Edwards et al. (2014b) use Bayesian model averaging to assign scores to model runs in
3 perturbed-parameter ensembles, but the scores in these methods are essentially based on RMSE
4 for low-dimensional summaries of model output and therefore do not fully account for the
5 spatial information in ice model output.

6 Here, we address these challenges using a Bayesian framework that combines data, models, and
7 prior beliefs about model input parameter values. Like McNeall et al. (2013), we train an
8 emulator on an ensemble of ice sheet model runs. However, we build on their work by using
9 an explicit likelihood function, and by incorporating information from a north-south profile of
10 average ice thicknesses. Specifically, we use a Gaussian process emulator to estimate the first
11 10 principal components of the zonal mean ice thickness profile, following a recent climate
12 model calibration study (Chang et al., 2013). Further, we perform a perfect model experiment
13 to investigate the interactions between input parameters. Our approach recovers the correct
14 parameter values and projected ice volume changes from an "assumed-true" model realization,
15 and the multi-dimensional probability density function displays expected physical interactions
16 (Section 1.2, below). These interactions were not evident from the simple analysis employed
17 by Applegate et al. (2012, their Fig. 1).

18 The above paragraphs discuss the case in which the ice sheet model is free to evolve to the state
19 that is most consistent with the selected parameter combination, the bedrock topography and
20 the climate (whether steady or varying). In such studies, parameters such as the basal sliding
21 coefficient are held constant over the geographic area of the ice sheet. However, a number of
22 recent studies (e.g., Shannon et al., 2013; Edwards et al., 2014b) have used an alternative
23 approach in which the spatially-distributed basal sliding coefficients and/or surface mass
24 balance fields are tuned so that the ice sheet model matches the observed modern geometry.
25 This approach has several advantages; the simulated modern ice sheet is guaranteed to match
26 the observed modern one, and the estimated basal sliding coefficients vary spatially, as is almost
27 certainly the case for the real ice sheet. However, such studies are silent on interactions between
28 parameters besides the basal sliding coefficient and surface mass balance, as we investigate
29 here.

30 The paper proceeds as follows. In the remainder of the Introduction, we describe the ensemble
31 that we use to train the emulator. In Section 2, we outline our method for using a Gaussian
32 process emulator to estimate the principal components of the zonally-averaged ice thicknesses,

1 and the setup of our perfect model experiment. Section 3 presents the results of the perfect
2 model experiment. In Section 4, we conclude by pointing out the implications of our work, as
3 well as its limitations and potential directions for future research.

4 **1.1 The ensemble**

5 We train our emulator with a 100-member perturbed-parameter ensemble described in
6 Applegate et al. (2012). This ensemble uses the three-dimensional ice sheet model SICOPOLIS
7 (Greve, 1997; Greve et al., 2011). Each model run spans the period from 125,000 years ago
8 (125 ka BP) to 3500, driven by surface temperature and sea level histories derived from
9 geologic data (Imbrie et al., 1984; Dansgaard et al., 1993; Johnsen et al., 1997) and forced into
10 the future with an asymptotic warming to $\sim 5^{\circ}\text{C}$ above present values. SICOPOLIS is a shallow
11 ice-approximation model, meaning that it neglects longitudinal stresses within the ice body
12 (Kirchner et al., 2011). Like most ice sheet models, it also includes many simplifications in
13 calculating the surface mass balance, notably through its use of the positive degree-day method
14 for relating surface temperatures to melting (Braithwaite, 1995; Calov and Greve, 2005; van
15 der Berg et al., 2011). These simplifications improve SICOPOLIS' computational efficiency
16 relative to higher-order or full-Stokes models (e.g., Seddik et al., 2012), allowing it to be run
17 repeatedly over 10^5 -yr time scales.

18 The parameter combinations in the Applegate et al. (2012) ensemble were chosen by Latin
19 hypercube sampling (McKay et al., 1979), following the earlier work of Stone et al. (2010).
20 Latin hypercube sampling distributes points throughout parameter space more efficiently than
21 Monte Carlo methods (Urban and Fricker, 2010). In their experiment, Applegate et al. (2012)
22 varied the ice flow enhancement factor, the ice and snow positive degree-day factors, the
23 geothermal heat flux, and the basal sliding factor (Ritz et al., 1997; cf. Stone et al., 2010;
24 Fitzgerald et al., 2011). These parameters control the softness of ice, the rapidity with which
25 the ice sheet's surface lowers at a given temperature, the amount of heat that enters the base of
26 the ice sheet, and the speed of sliding at a given stress (see Applegate et al., 2012, for an
27 explanation of how each parameter affects model behavior).

28 McNeall et al. (2013) trained their emulator using a perturbed-parameter ensemble of ice sheet
29 model runs published by Stone et al. (2010). Key differences between the Applegate et al.
30 (2012) ensemble and the Stone et al. (2010) ensemble involve the parameters varied in the
31 ensembles and the processes included in the simulations. Stone et al. (2010) varied the lapse

1 rate instead of the basal sliding factor adjusted by Applegate et al. (2012). The model used by
2 Stone et al. (2010; Glimmer v. 1.0.4; see Rutt et al., 2009) neglects basal sliding, a process
3 included in the SICOPOLIS runs presented by Applegate et al. (2012).

4 The results presented by Applegate et al. (2012) suggest that widely diverging ice sheet model
5 parameter values yield comparable modern ice sheets, but substantially different sea level rise
6 projections. Applegate et al. (2012) assessed the plausibility of their model runs by comparing
7 the simulated ice volumes in 2005 to the estimated modern ice volume (Bamber et al., 2001;
8 Lemke et al., 2007); those runs that yielded modern ice volumes within 10% of the estimated
9 value were kept. These plausible runs yielded a range of future sea level rise projections that
10 was ~75% of the median estimate.

11 Moreover, the parameter combinations that agree well with the modern ice volume constraint
12 are widely distributed over parameter space. With the exception of the ice positive degree-day
13 factor, where only values less than $\sim 15 \text{ mm day}^{-1} \text{ }^{\circ}\text{C}^{-1}$ satisfy the ice volume constraint, no
14 pattern emerges from the distribution of the successful runs through parameter space. McNeall
15 et al. (2013) make a similar point using their own results. Statistically, this inability to learn
16 about the plausibility of various parameter combinations given observations is termed an
17 "identifiability problem."

18 **1.2 Expected interactions among model input parameters**

19 The apparently-structureless distribution of successful runs through parameter space
20 (Applegate et al., 2012, their Fig. 1) may stem from interactions among the parameters. The
21 parameters can be loosely grouped into those that control the ice sheet's surface mass balance
22 (the ice and snow positive degree-day factors) and those that control ice movement (the ice flow
23 enhancement factor, the basal sliding factor, and the geothermal heat flux). Either group of
24 parameters can cause mass loss from the ice sheet to be high or low, given fixed values of the
25 parameters in the other group. For example, a high ice positive degree-day factor should be
26 associated with a low snow positive degree-day factor to produce the same amount of melt as
27 a model run with more moderate values of both parameters. This interaction is bounded,
28 however, because the maximum snow positive degree-day factor is much lower than the
29 maximum value for ice; also, at the peak of the ablation season, there is no snow left on the
30 lower parts of the ice sheet, so the ice positive degree-day factor dominates over part of the
31 year. Similarly, the same ice velocities can be produced by either a high flow enhancement

1 factor and a low basal sliding factor, or the reverse. Basal sliding can be a much faster process
2 than ice flow, so this parameter interaction is also bounded. However, basal sliding operates
3 only where the bed is thawed, and the geothermal heat flux likely controls the fraction of the
4 bed that is above the pressure melting point.

5 The relatively small number of design points in the ensemble presented by Applegate et al.
6 (2012) hinders mapping of the interactions among parameters over their five-dimensional
7 space. Coherent mapping requires many more design points, but performing these additional
8 runs with the full ice sheet model is impractical because of the model's high computational cost.
9 This problem suggests a need for a computationally efficient emulator to fill the gaps in
10 parameter space between the existing model runs.

11

12 **2 Methods**

13 As described above, our goals are 1) to present a method for quantifying the agreement between
14 ice sheet model output and observations that incorporates spatial information, 2) to characterize
15 the interactions among input parameters, and 3) to produce illustrative projections of sea level
16 rise from the Greenland Ice Sheet based on synthetic data. In this section, we provide an outline
17 of our methods for achieving these goals; fuller descriptions appear in Chang et al. (2013) and
18 in the Supporting Information.

19 We accomplish goal #1 through constructing a statistical model that results in a likelihood
20 function. This statistical model compares ice sheet model output and observations to evaluate
21 the plausibility of a vector of model input parameter values Θ while accounting for systematic
22 discrepancies between the model output and the observations. The likelihood function for the
23 ice thickness observations, denoted by Z , is based on the additive model

$$24 \quad Z = Y(\Theta) + \delta + \epsilon, \quad (1)$$

25 where $Y(\Theta)$ is the ice thickness output from SICOPOLIS model at the vector of input parameter
26 values Θ , δ is the discrepancy between model output and observations caused by structural
27 problems in the model, and ϵ is independently- and identically-distributed observational noise.
28 To achieve goal #2, we perform a "leave-one-out" perfect model experiment with a Gaussian

1 process emulator, a computationally-cheap surrogate for the full ice sheet model. As described
2 above, the model output $\mathbf{Y}(\boldsymbol{\theta})$ is available only at a relatively small number of points in
3 parameter space, and therefore it is necessary to build an emulator that approximates the model
4 output $\mathbf{Y}(\boldsymbol{\theta})$ at any given $\boldsymbol{\theta}$.

5 Direct emulation of the full two-dimensional ice thickness grid is prohibitively expensive, due
6 to (i) the cost of performing operations on large covariance matrices (see the Supplementary
7 Information and Chang et al., 2013, for details) and (ii) the need to model spatial processes that
8 contain many zeros, which poses non-trivial computational and inferential challenges. To
9 mitigate these problems, we take the mean of each row in the ice thickness grid, thereby
10 obtaining a 264-element vector of zonally-averaged ice thicknesses for each ice sheet model
11 run. We then apply principal component analysis to these mean ice thickness vectors. The
12 magnitudes of the first 10 principal components suffice to recover the mean ice thickness
13 vectors. Because the principal components are uncorrelated, we can construct a separate
14 emulator for the magnitude of each principal component. Our emulator consists of all these
15 independent Gaussian processes. Although our emulator operates in the principal component
16 space, we can reconstruct the ice thickness profile that corresponds to the emulated principal
17 components (see the Supporting Information for details). Note that our likelihood formulation
18 automatically penalizes the components with lower explained variation.

19 Next, we train the emulator on all but one of the model runs. We refer to the output (specifically,
20 the zonal mean ice thickness profile and the ice volume change projection) from this left-out
21 model run as our "assumed truth." We examined the robustness of our methods by successively
22 leaving out each model run in turn and repeating our analysis; see the Supplementary
23 Information.

24 Before using the mean ice thickness profile from our assumed-true model run in our perfect
25 model experiment, we contaminate it with spatially-correlated errors. These errors reflect the
26 discrepancies that we would expect to see between model output and data in a "real" calibration
27 experiment, due to missing or parameterized processes in the model. In particular, we use
28 spatially-correlated errors with a moderate magnitude (standard deviation of 50 m) and a large-
29 scale spatial trend to represent a situation in which (i) the ice sheet model has reasonable skill
30 in reproducing the observed spatial pattern of modern ice thickness, and (ii) the discrepancy
31 pattern is notably different from patterns generated by the ice sheet model and is therefore

1 statistically identifiable (see the Supplementary Information for more details). Note that any
2 probabilistic calibration method, including our approach, can be uninformative if condition (i)
3 is violated, or subject to serious bias if condition (ii) is violated.

4 We then use Markov chain Monte Carlo (MCMC) to estimate the joint posterior probability
5 distribution over the five-dimensional input parameter space. MCMC is a well-established
6 (Hastings, 1970), but complex, statistical technique; Brooks et al. (2011) provide a book-length
7 treatment. Briefly, the Metropolis-Hastings algorithm used in MCMC constructs a sequence of
8 parameter combinations, each of which is chosen randomly from the region of parameter space
9 surrounding the last point. Candidate parameter combinations are accepted if the posterior
10 probability of the new point is greater than at the previous one, or with a certain probability
11 determined by the Metropolis-Hastings acceptance ratio otherwise. If the candidate point is
12 rejected, another candidate point is chosen at random according to a proposal distribution.
13 Consistent with McNeall et al. (2013), we match the emulator estimates to assumed-true model
14 output instead of observed ice thickness values (Bamber et al., 2001, 2013) because a perfect
15 model experiment is more suitable to achieve our main objectives, studying and demonstrating
16 the performance of our probabilistic calibration method. The candidate points that are retained
17 by the MCMC algorithm approximate the posterior probability distribution of the input
18 parameter space. The candidate points from this algorithm therefore reflect various
19 characteristics of the posterior distribution, including the marginal distributions of each of the
20 parameters separately and their joint distributions. Hence, we can use MCMC to summarize
21 what we have learned about the parameters from the model and observations while accounting
22 for various uncertainties and prior information.

23 Finally, to achieve goal #3, we use a separate Gaussian process emulator to interpolate between
24 the ice volume change projections from all the model runs in the original ensemble (Applegate
25 et al., 2012), except the assumed-true realization. When applied to the sample of the model
26 input parameters that we obtained from Markov chain Monte Carlo, this emulator yields a
27 sample of ice volume changes, and thus sea level rise contributions, between 2005 and 2100.
28 We then use kernel density estimation to compute the probability density of the projected sea
29 level rise contributions. It should be noted that these projections are based on synthetic data
30 (not real observations), and do not represent "real" projections of Greenland Ice Sheet mass loss
31 over this century.

32

1 **3 Results**

2 Besides helping to diagnose interactions among ice sheet model parameters, our perfect model
3 experiment allows us to test our overall procedure. We carry out several checks.

4 1) If the trained emulator is given the parameter settings from the left-out model realization, it
5 should produce a close approximation to the actual output from that realization.

6 2) The maximum of the multidimensional posterior probability function from our Markov chain
7 Monte Carlo analysis should lie close to the parameter settings from the left-out model
8 realization.

9 3) The mode of the probability density function of ice loss projections should be close to the
10 ice loss projection from the assumed-true model realization.

11 As detailed below, our methods pass all three of these checks.

12 Aggregating the ice thicknesses to their zonal means allows easy visual comparison of different
13 emulator-estimated ice thickness vectors to the assumed-true model realization (black curve,
14 Fig. 1). The emulator, as trained on 99 of the model realizations from the Applegate et al. (2012)
15 ensemble, successfully recovers the ice thicknesses from the left-out model realization (Fig. 2)
16 when given the parameter combination for that left-out model realization as input. Differences
17 between the assumed-true and emulated zonally-averaged ice thickness vectors are minor. Thus,
18 our methods pass check #1, above.

19 Similarly, the conditional posterior density functions (Fig. 3) have maxima near the assumed-
20 true parameter values. Parameter combinations yielding zonally-averaged ice thickness curves
21 that lie close to the assumed-true model realization (e.g., the red curve in Fig. 1) are more likely
22 (more probable based on the posterior distribution) than those with curves that lie farther from
23 the assumed-true values (blue and green curves in Fig. 1). We do not expect that the modes of
24 the marginal posterior density functions (Fig. 4b) will fall exactly at the assumed-true parameter
25 values, because summing over one or more dimensions often moves the marginal mode away
26 from the maximum of the multidimensional probability density function. In any case, the
27 maximum posterior probability is close to the assumed-true parameter combination. Thus, our
28 methods pass check #2, above. Some of the two-dimensional marginal probability density
29 functions (Fig. 4b) show multiple modes and bands of high probability extending across the
30 two-dimensional fields; we discuss the significance of these features below.

1 For comparison, we also produced scatterplots of parameter combinations as projected onto
2 two-dimensional slices through the five-dimensional parameter space (Fig. 4a), following
3 Applegate et al. (2012, their Fig. 1). As in Applegate et al. (2012), the "successful" design
4 points show no clustering around the assumed-true parameter values, except for the ice PDD
5 factor.

6 Our method also successfully recovers the ice volume loss produced by the assumed-true model
7 realization (Fig. 5; see also Figs. S3, S4), reflected by the close correspondence between the
8 mode of the probability density function produced by our methods and the vertical black line.
9 Thus, our methods pass check #3, listed above. As previously noted, these projections are based
10 on synthetic data; they are not "real" projections of Greenland Ice Sheet mass loss. For
11 comparison, we also applied the windowing approach used by Applegate et al. (2012) to the
12 model runs and the synthetic observation. The 95% probable interval produced by our methods
13 is much smaller than that estimated by computing the 2.5th and the 97.5th percentiles of the
14 volume change values selected by the 10% volume filter used in Applegate et al. (2012). This
15 reflects the utility of spatial information and our probabilistic calibration approach in reducing
16 projection uncertainties comparing to the windowing approach in Applegate et al. (2012).

17 The prior density for the ice volume loss was constructed by assuming that all 99 design points
18 used to train our emulator are equally likely. Interestingly, a uniform prior for the input
19 parameters results in a skewed and multimodal prior distribution for the volume loss, indicating
20 that the function that maps input parameters to projected ice volume changes is highly non-
21 linear and not smooth. These characteristics also cause a small offset between the assumed-
22 true projection and the mode of the posterior density. The marginal plots for the volume loss
23 projection surfaces are shown in Figure S1 in the supporting material.

24

25 **4 Discussion**

26 As explained above, our goals for this work were to identify an objective function for matching
27 ice sheet models to spatially-distributed data (especially ice thicknesses), map interactions
28 among model input parameters, and develop methods for projecting future ice sheet mass loss,
29 with well-characterized uncertainties. We demonstrated that our emulator reproduces a vector
30 of zonally-averaged ice thicknesses from a given model run when trained on other members
31 from the same ensemble (Fig. 2). We further showed that the emulator can recover the
32 appropriate parameter combinations for an assumed-true model realization in a perfect model

1 experiment (Figs. 3, 4b). Finally, we produced illustrative projections of Greenland Ice Sheet
2 mass loss, based on synthetic data (Fig. 5; see also Figs. S3, S4). As noted above, our
3 projections are for illustration only, and do not represent "real" projections of future Greenland
4 Ice Sheet mass loss.

5 The utility of our approach becomes clear in comparing the marginal posterior probability
6 density functions (Fig. 4a) and projections (red probability density functions and boxplots in
7 Figs. 5, S3, and S4) to results from simpler methods (Fig. 4b; blue boxplots in Figs. 5, S3, and
8 S4; Applegate et al., 2012). In Figure 4b, there are distinct modes in the marginal densities,
9 indicating regions of parameter space that are more consistent with the assumed truth. These
10 modes are absent in the simpler graphic (Fig. 4a). Similarly, the 95% probable interval of sea
11 level rise contributions is narrower using our methods than if a simple windowing approach is
12 applied (Fig. 5; see also Figs. S3, S4). Our results also show the importance of including the
13 discrepancy term (δ in Eqn. 1) for recovering the appropriate parameter settings in our perfect
14 model experiments (Fig. S2). If we leave this discrepancy term out, the marginal posterior
15 density functions for each parameter clearly miss the true values.

16 The parameter interactions identified in this experiment are generally consistent with intuition
17 (see Section 1.2 for descriptions of anticipated parameter interactions). Figure 4 shows inclined
18 bands of high marginal posterior probability in the ice positive degree-day vs. snow positive
19 degree-day, geothermal heat flux vs. ice flow factor, and basal sliding factor vs. flow factor
20 panels. As expected, there are tradeoffs among each of these parameter pairs; for example, a
21 low ice positive degree-day factor must be combined with a high snow positive degree-day
22 factor to produce a reasonable match to the assumed truth. Somewhat surprisingly, the tradeoff
23 between the geothermal heat flux and the ice flow factor is much stronger than that between the
24 geothermal heat flux and the basal sliding factor. The geothermal heat flux affects both ice
25 deformation (which is temperature-sensitive) and basal sliding (which operates only where
26 there is liquid water at the ice-bed interface). We hypothesize that the geothermal heat flux has
27 a stronger effect on ice flow than basal sliding because ice deformation happens over a much
28 larger fraction of the ice sheet's basal area than does sliding.

29 Multiple modes appear in the two-dimensional marginal density plots (Fig. 4), implying that
30 standard methods for tuning of ice sheet models may converge to "non-optimal" parameter
31 combinations. Ice sheet models are commonly tuned by manually adjusting one parameter at a
32 time until the simulated modern ice sheet resembles the real one (e.g., Greve et al., 2011). This

1 procedure is an informal variant of so-called gradient descent methods, which search for
2 optimal matches between models and data by moving down a continuous surface defined by
3 the model's input parameters, the objective function, and the data. If the surface has multiple
4 "peaks" (i.e. regions of parameter space that are more plausible, given observations, than their
5 surroundings), gradient descent methods can converge to a point which produces a better match
6 to the data than any adjacent point, but is nevertheless far from the "best" parameter
7 combination. This problem may partly explain the wide variation in projections of sea level
8 rise from the ice sheets, as made with state-of-the-art ice sheet models (Bindschadler et al.,
9 2013; cf. Shannon et al., 2013; Edwards et al., 2014a): even if the models had similar structures
10 and reproduced the modern ice sheet topography and ice thicknesses equally well, we would
11 still expect their future projections to diverge because of differences in input parameter choice.
12 Our leave-one-out cross-validation shows that the results presented here are consistent across
13 all possible 100 synthetic truths. The prediction interal for the ice volume changes in Fig 5
14 achieves the nominal coverage when the synthetic truth yields a modern ice volume that is close
15 to the observed modern ice volume (Fig. S5). The parameter interactions shown in Fig. 4 are
16 also consistent across the majority of the synthetic truths (Fig. S6).

17 **4.1 Cautions and future directions**

18 In this paper, we specifically avoid giving "real" projections of future Greenland Ice Sheet
19 volume change, for two reasons. First, we match only a two-dimensional profile of zonally-
20 averaged ice thicknesses from an assumed-true model run, rather than the two-dimensional grid
21 of observed ice thicknesses (Bamber et al., 2001, 2013; see also McNeall et al., 2013). Second,
22 the ensemble of ice sheet model runs (Applegate et al., 2012) that we use to calibrate our
23 emulator has several important limitations, including the relative simplicity of the model used
24 to generate the ensemble and the synthetic climate scenario used to drive the ensemble members
25 into the future. Most importantly, this ensemble's simulated modern ice sheets are generally
26 too thick in the southern part of Greenland and too thin in the northern part of the island
27 (Applegate et al., 2012, their Fig. 7); other studies that allow the ice sheet surface to evolve
28 freely have noted similar difficulties in reproducing the modern ice sheet (e.g., Stone et al.,
29 2010; Greve et al., 2011; Nowicki et al., 2013, their Fig. 2; cf. Edwards et al., 2014a). The long-
30 term goal of this work is to compare ice sheet model runs to actual data, thereby resulting in
31 probabilistic projections of future ice sheet mass loss. To achieve this goal, we plan to expand
32 our method to treat the full, two-dimensional ice thickness grid and take advantage of other

1 spatially-distributed data sets (e.g., surface velocities; Joughin et al. 2010), and to generate new
2 ice sheet model ensembles that overcome the limitations explained above.

3

4 **5 Conclusions**

5 In this paper, we presented an approach for probabilistic calibration of ice sheet models using
6 spatially-resolved ice thickness information. Specifically, we constructed a probability model
7 for assigning posterior probabilities to individual ice sheet model runs, and we used a Gaussian
8 process emulator to interpolate between existing ice sheet model simulations. We reduced the
9 dimensionality of the emulation problem by reducing profiles of mean ice thicknesses to their
10 principal components. Finally, we showed how the posterior probabilities from the model
11 calibration exercise can be used to make projections of future sea level rise from the ice sheets.
12 In a perfect model experiment where the "true" parameter settings and future contributions of
13 the ice sheet to sea level rise are known, our methods successfully recovered these values. The
14 posterior probability density function that resulted from this experiment shows tradeoffs among
15 parameters and multiple modes. The tradeoffs are consistent with physical expectations,
16 whereas the multiple modes may indicate that commonly-applied methods for tuning ice sheet
17 models can lead to calibration errors.

18

19 **Acknowledgements**

20 We thank R. Greve for distributing his ice sheet model SICOPOLIS freely on the Web
21 (<http://sicopolis.greveweb.net/>), and N. Kirchner for help in setting up and using the model. R.
22 Alley and D. Pollard provided helpful comments on a draft of the manuscript. This work was
23 partially supported by the US Department of Energy, Office of Science, Biological and
24 Environmental Research Program, Integrated Assessment Program, Grant No. DE-SC0005171;
25 by the US National Science Foundation through the Network for Sustainable Climate Risk
26 Management (SCRiM) under NSF cooperative agreement GEO-1240507; and by the Penn
27 State Center for Climate Risk Management. Any opinions, findings, and conclusions expressed
28 in this work are those of the authors, and do not necessarily reflect the views of the National
29 Science Foundation or the Department of Energy. Supplementary material related to this article
30 is available online at <http://www.geosci-model-dev-discuss.net/7/1905/2014/> gmdd-7-1905-
31 2014-supplement.pdf.

1 **Author Contributions**

2 WC designed the emulator, carried out the analyses, and wrote the first draft of the
3 Supplementary Information. PJA wrote the first draft of the body text and supplied the
4 previously-published ice sheet model runs (available online at
5 <http://bolin.su.se/data/Applegate-2011>). WC, PJA, MH, and KK jointly designed the research
6 and edited the paper text.

7

1 **References**

2 Alley, R. B., Andrews, J. T., Brigham-Grette, J., Clarke, G. K. C., Cuffey, K. M., Fitzpatrick,
3 J. J., Funder, S., Marshall, S. J., Miller, G. H., Mitrovica, J. X., Muhs, D. R., Otto-Bliesner, B.
4 L., Polyak, L., and White, J. W. C.: History of the Greenland Ice Sheet: paleoclimatic insights,
5 Quaternary Sci. Rev., 29, 1728–1756, 2010.

6 Applegate, P. J., Kirchner, N., Stone, E. J., Keller, K., and Greve, R.: An assessment of key
7 model parametric uncertainties in projections of Greenland Ice Sheet behavior, The Cryosphere,
8 6, 589–606, doi:10.5194/tc-6-589-2012, 2012.

9 Alexander, L. V., Allen, S. K., Bindoff, N. L., Bron, F. M., Church, J. A., Cubasch, U., Emori,
10 S., Forster, P., Friedlingstein, P., Gillett, N., Gregory, J. M., Hartmann, D. L., Jansen, E.,
11 Kirtman, B., Knutti, R., Kanikicharla, K. K., Lemke, P., Marotzke, J., Masson-Delmotte, V.,
12 Meehl, G. A., Mokhov, I. I., Piao, S., Plattner, G. K., Dahe, Q., Ramaswamy, V., Randall, D.,
13 Rhein, M., Rojas, M., Sabine, C., Shindell, D., Stocker, T. F., Talley, L. D., Vaughan, D. G.
14 and Xie, S. P. (2013). Climate Change 2013: The Physical Science Basis: Contribution of
15 Working Group I to the Fifth Assessment Report of the Intergovernmental Panel on Climate
16 Change. IPCC, Cambridge University Press, Cambridge.

17 Bamber, J. L. and Aspinall, W. P.: An expert judgement assessment of future sea level rise from
18 the ice sheets, Nature Clim. Change, 3, 424–427, 2013.

19 Bamber, J. L., Layberry, R. L., and Gogineni, S. P.: A new ice thickness and bed data set for
20 the Greenland ice sheet 1. Measurement, data reduction, and errors, J. Geophys. Res., 106,
21 33773–33780, 2001.

22 Bamber, J. L., Griggs, J. A., Hurkmans, R. T. W. L., Dowdeswell, J. A., Gogineni, S. P., Howat,
23 I., Mouginot, J., Paden, J., Palmer, S., Rignot, E., and Steinhage, D.: A new bed elevation
24 dataset for Greenland, The Cryosphere, 7, 499–510, doi:10.5194/tc-7-499-2013, 2013.

25 Bindschadler, R. A., Nowicki, S., Abe-Ouchi, A., Aschwanden, A., Choi, H., Fastook,
26 J., Granzow, G., Greve, R., Gutowski, G., Herzfeld, U., Jackson, C., Johnson, J., Khroulev, C.,
27 Levermann, A., Lipscomb, W. H., Martin, M. A., Morlighem, M., Parizek, B. R., Pollard, D.,
28 Price, S. F., Ren, D., Saito, F., Sato, T., Seddik, H., Seroussi, H., Takahashi, K., Walker, R.,
29 and Wang, W. L.: Ice-sheet model sensitivities to environmental forcing and their use in
30 projecting future sea level (the SeaRise project), J. Glaciol., 59, 195–224, 2013.

1 Born, A. and Nisancioglu, K. H.: Melting of Northern Greenland during the last interglaciation,
2 The Cryosphere, 6, 1239–1250, doi:10.5194/tc-6-1239-2012, 2012.

3 Braithwaite, R. J.: Positive degree-day factors for ablation on the Greenland ice sheet studied
4 by energy-balance modelling, J. Glaciol., 41, 153–160, 1995.

5 Brooks, S., Gelman, A., Jones, G., and Meng, X.-L. (Eds.): Handbook of Markov Chain Monte
6 Carlo, Chapman and Hall/CRC, 619 pp., 2011.

7 Calov, R. and Greve, R.: A semi-analytical solution for the positive degree-day model with
8 stochastic temperature variations, J. Glaciol., 51, 173–175, 2005.

9 Chang, W., Haran, M., Olson, R., and Keller, K.: Fast dimension-reduced climate model
10 calibration, Ann. Appl. Stat., accepted, 2014.

11 Church, J. A. and White, N. J.: A 20th century acceleration in global sea-level rise, Geophys.
12 Res. Lett., 33, L01602, doi:10.1029/2005GL024826, 2006.

13 Cuffey, K. M. and Kavanaugh, J. L.: How nonlinear is the creep deformation of polar ice? A
14 new field assessment, Geology, 39, 1027–1030, 2011.

15 Edwards, TL, Fettweis, X, Gagliardini, O, Gillet-Chaulet, F, Goelzer, H, Gregory, J, Hoffman,
16 M, Huybrechts, P, Payne, AJ, Perego, M, Price, S, Quiquet, A & Ritz, C: Effect of uncertainty
17 in surface mass balance–elevation feedback on projections of the future sea level contribution
18 of the Greenland ice sheet. The Cryosphere, 8, 195-208 doi:10.5194/tc-8-195-2014, 2014a

19 Edwards, TL, Fettweis, X, Gagliardini, O, Gillet-Chaulet, F, Goelzer, H, Gregory, J, Hoffman,
20 M, Huybrechts, P, Payne, AJ, Perego, M, Price, S, Quiquet, A & Ritz, C: Probabilistic
21 parameterisation of the surface mass balance elevation feedback in regional climate model
22 simulations of the Greenland ice sheet. The Cryosphere, 8, 181-194 doi:10.5194/tc-8-181-2014,
23 2014b

24 Fitzgerald, P. W., Bamber, J. L., Ridley, J. K., and Rougier, J. C.: Exploration of parametric
25 uncertainty in a surface mass balance model applied to the Greenland ice sheet, J. Geophys.
26 Res., 117, F01021, doi:10.1029/2011JF002067, 2012.

27 Fyke, J. G., Weaver, A. J., Pollard, D., Eby, M., Carter, L., and Mackintosh, A.: A new coupled
28 ice sheet/climate model: description and sensitivity to model physics under Eemian, Last
29 Glacial Maximum, late Holocene and modern climate conditions, Geosci. Model Dev., 4, 117–
30 136, doi:10.5194/gmd-4-117-2011, 2011.

1 Greve, R.: Application of a polythermal three-dimensional ice sheet model to the Greenland Ice
2 Sheet: response to steady-state and transient climate scenarios, *J. Climate*, 10, 901–918, 1997.

3 Greve, R. and Otsu, S.: The effect of the north-east ice stream on the Greenland ice sheet in
4 changing climates, *The Cryosphere Discuss.*, 1, 41–76, doi:10.5194/tcd-1-41-2007, 2007.

5 Greve, R., Saito, F., and Abe-Ouchi, A.: Initial results of the SeaRISE numerical experiments
6 with the models SICOPOLIS and IcIES for the Greenland Ice Sheet, *Ann. Glaciol.*, 52, 23–30,
7 2011.

8 Grinsted, A., Moore, J. C., and Jevrejeva, S.: Reconstructing sea level from paleo and projected
9 temperatures, 200 to 2100 AD, *Clim. Dynam.*, 34, 461–472, doi:10.1007/s00382-008-0507-2,
10 2009.

11 Hastings, W. K.: Monte Carlo sampling methods using Markov chains and their applications,
12 *Biometrika*, 57, 97–109, 1970.

13 Hebeler, F., Purves, R. S., and Jamieson, S. S. R.: The impact of parametric uncertainty and
14 topographic error in ice-sheet modelling, *J. Glaciol.*, 54, 899–919, 2008.

15 Heimbach, P. and Bugnion, V.: Greenland ice-sheet volume sensitivity to basal, surface and
16 initial conditions derived from an adjoint model, *Ann. Glaciol.*, 50, 67–80, 2009.

17 Huybrechts, P.: Sea-level changes at the LGM from ice-dynamic reconstructions of the
18 Greenland and Antarctic ice sheets during the glacial period, *Quaternary Sci. Rev.*, 21, 203–
19 231, 2002.

20 Jevrejeva, S., Moore, J. C., Grinsted, A., and Woodworth, P. L.: Recent global sea level
21 acceleration started over 200 years ago?, *Geophys. Res. Lett.*, 35, L08715,
22 doi:10.1029/2008GL033611, 2008.

23 Jevrejeva, S., Moore, J. C., and Grinsted, A.: Sea level projections to AD2500 with a new
24 generation of climate change scenarios, *Global Planet. Change*, 80–81, 14–20, 2012.

25 Joughin, I., Smith, B. E., Howat, I. M., Scambos, T., and Moon, T.: Greenland flow variability
26 from ice-sheet-wide velocity mapping, *J. Glaciol.*, 56, 415–430, 2010. Kennedy, M. C. and
27 O'Hagan, A.: Bayesian calibration of computer models, *J. R. Statist. Soc. B*, 63, 425–464, 2001.

28 Kirchner, N., Hutter, K., Jakobsson, M., and Gyllencreutz, R.: Capabilities and limitations of
29 numerical ice sheet models: a discussion for Earth-scientists and modelers, *Quaternary Sci.*
30 *Rev.*, 30, 3691–3704, 2011.

1 Lemke, P., Ren, J., Alley, R. B., Allison, I., Carrasco, J., Flato, G., Fujii, Y., Kaser, G., Mote,
2 P., Thomas, R. H., and Zhang, T.: Observations: changes in snow, ice, and frozen ground, edited
3 by: Solomon, S., Qin, D., Manning, M., Chen, Z., Marquis, M., Averyt, K. B., Tignor, M., and
4 Miller, H. L., Cambridge University Press, Cambridge, 2007.

5 Lempert, R., Srivastava, R. L., and Keller, K.: Characterizing uncertain sea level rise projections to
6 support investment decisions, California Energy Commission Report CEC-500-2012-056, 2012.

7 Lenton, T. M., Held, H., Kriegler, E., Hall, J. W., Lucht, W., Rahmstorf, S., and Schnellhuber,
8 H. J.: Tipping elements in the Earth's climate system, *P. Natl. Acad. Sci. USA*, 105, 1786–1793,
9 2008.

10 Little, C. M., Oppenheimer, M., Urban, N. M.: Upper bounds on twenty-first-century Antarctic
11 ice loss assessed using a probabilistic framework, *Nature Climate Change* 3, 654–659,
12 doi:10.1038/nclimate1845, 2013

13 McKay, M. D., Beckman, R. J., and Conover, W. J.: A comparison of three methods for
14 selecting values of input variables in the analysis of output from a computer code,
15 *Technometrics*, 21, 239–245, 1979.

16 McNeall, D. J., Challenor, P. G., Gattiker, J. R., and Stone, E. J.: The potential of an
17 observational data set for calibration of a computationally expensive computer model, *Geosci.
18 Model Dev.*, 6, 1715–1728, doi:10.5194/gmd-6-1715-2013, 2013.

19 Meehl, G. A., Stocker, T. F., Collins, W. D., Friedlingstein, P., Gaye, A. T., Gregory, J. M.,
20 Kitoh, A., Knutti, R., Murphy, J. M., Noda, A., Raper, S. C. B., Watterson, I. G., Weaver, A.
21 J., and Zhao, Z.-C.: Global climate projections, edited by: Solomon, S., Qin, D., Manning, M.,
22 Chen, Z., Marquis, M., Averyt, K. B., Tignor, M., and Miller, H. L., Cambridge University
23 Press, Cambridge, 2007.

24 Nowicki, S., Bindschadler, R. A., Abe-Ouchi, A., Aschwanden, A., Bueler, E., Choi, H.,
25 Fastook, J., Granzow, G., Greve, R., Gutowski, G., Herzfeld, U., Jackson, C., Johnson, J.,
26 Khroulev, C., Larour, E., Levermann, A., Lipscomb, W. H., Martin, M. A., Morlighem, M.,
27 Parizek, B. R., Pollard, D., Price, S. F., Ren, D., Rignot, E., Saito, F., Sato, T., Seddik, H.,
28 Seroussi, H., Takahashi, K., Walker, R., and Wang, W. L.: Insights into spatial sensitivities of
29 ice mass response to environmental change from the SeaRISE ice sheet modeling project II:
30 Greenland, *J. Geophys. Res.-Earth*, 118, 1025–1044, doi:10.1002/jgrf.20076, 2013.

1 Pfeffer, W. T., Harper, J. T., and O'Neel, S.: Kinematic constraints on glacier contributions to
2 21st-century sea-level rise, *Nature*, 321, 1340–1343, 2008.

3 Pollard, D. and DeConto, R. M.: A simple inverse method for the distribution of basal sliding
4 coefficients under ice sheets, applied to Antarctica, *The Cryosphere*, 6, 953–971,
5 doi:10.5194/tc-6-953-2012, 2012.

6 Rahmstorf, S.: A semi-empirical approach to projecting future sea-level rise, *Science*, 315, 368–
7 370, 2007.

8 Ritz, C., Fabre, A., and Letreguilly, A.: Sensitivity of a Greenland Ice Sheet model to ice flow
9 and ablation parameters: consequences for the evolution through the last climatic cycle, *Clim.*
10 *Dynam.*, 13, 11–24, 1997.

11 Robinson, A., Calov, R., and Ganopolski, A.: An efficient regional energy-moisture balance
12 model for simulation of the Greenland Ice Sheet response to climate change, *The Cryosphere*,
13 4, 129–144, doi:10.5194/tc-4-129-2010, 2010.

14 Rutt, I. C., Haggdorn, M., Hulton, N. R. J., and Payne, A. J.: The Glimmer community ice-sheet
15 model, *J. Geophys. Res.-Earth*, 114, F02004, doi:10.1029/2008JF001015, 2009.

16 Sacks, J., Welch, W. J., Mitchell, T. J., and Wynn, H. P.: Design and analysis of computer
17 experiments (with discussion), *J. Stat. Sci.*, 4, 409–423, 1989.

18 Seddik, H., Greve, R., Zwinger, T., Gillet-Chaulet, F., and Gagliardini, O.: Simulations of the
19 Greenland ice sheet 100 years into the future with the full Stokes model Elmer/Ice, *J. Glaciol.*,
20 58, 427–440, 2012.

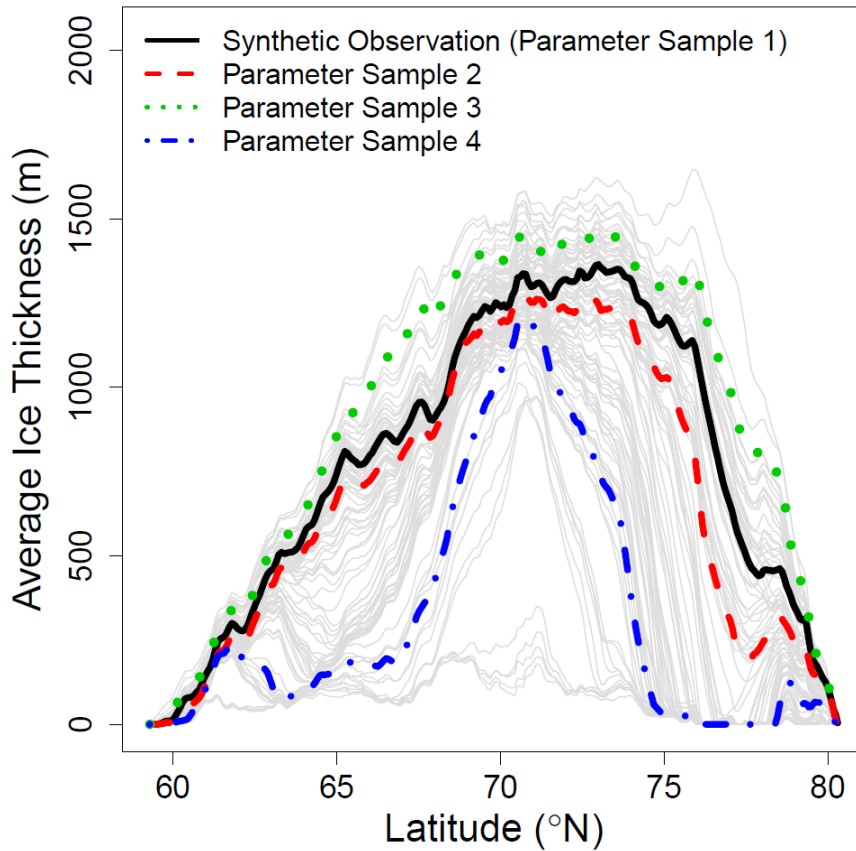
21 Stone, E. J., Lunt, D. J., Rutt, I. C., and Hanna, E.: Investigating the sensitivity of numerical
22 model simulations of the modern state of the Greenland ice-sheet and its future response to
23 climate change, *The Cryosphere*, 4, 397–417, doi:10.5194/tc-4-397-2010, 2010.

24 Urban, N. M. and Fricker, T. E.: A comparison of Latin hypercube and grid ensemble designs
25 for the multivariate emulation of an Earth system model, *Comput. Geosci.*, 36, 746–755, 2010.

26 van der Berg, W. J., van den Broeke, M., Ettema, J., van Meijgaard, E., and Kaspar, F.:
27 Significant contribution of insolation to Eemian melting of the Greenland ice sheet, *Nat. Geosci.*,
28 4, 679–683, 2011.

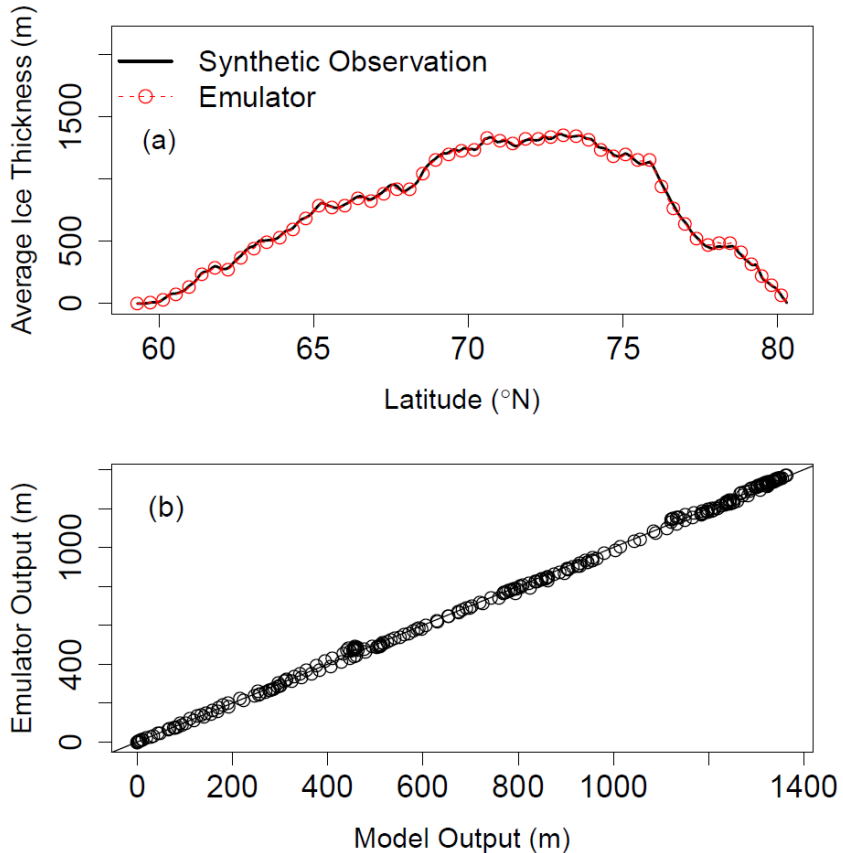
1 Vizcaino, M., Mikolajewicz, U., Jungclaus, J., and Schurgers, G.: Climate modification by
2 future ice sheet changes and consequences for ice sheet mass balance, *Clim. Dynam.*, 34, 301–
3 324, 2010.

4



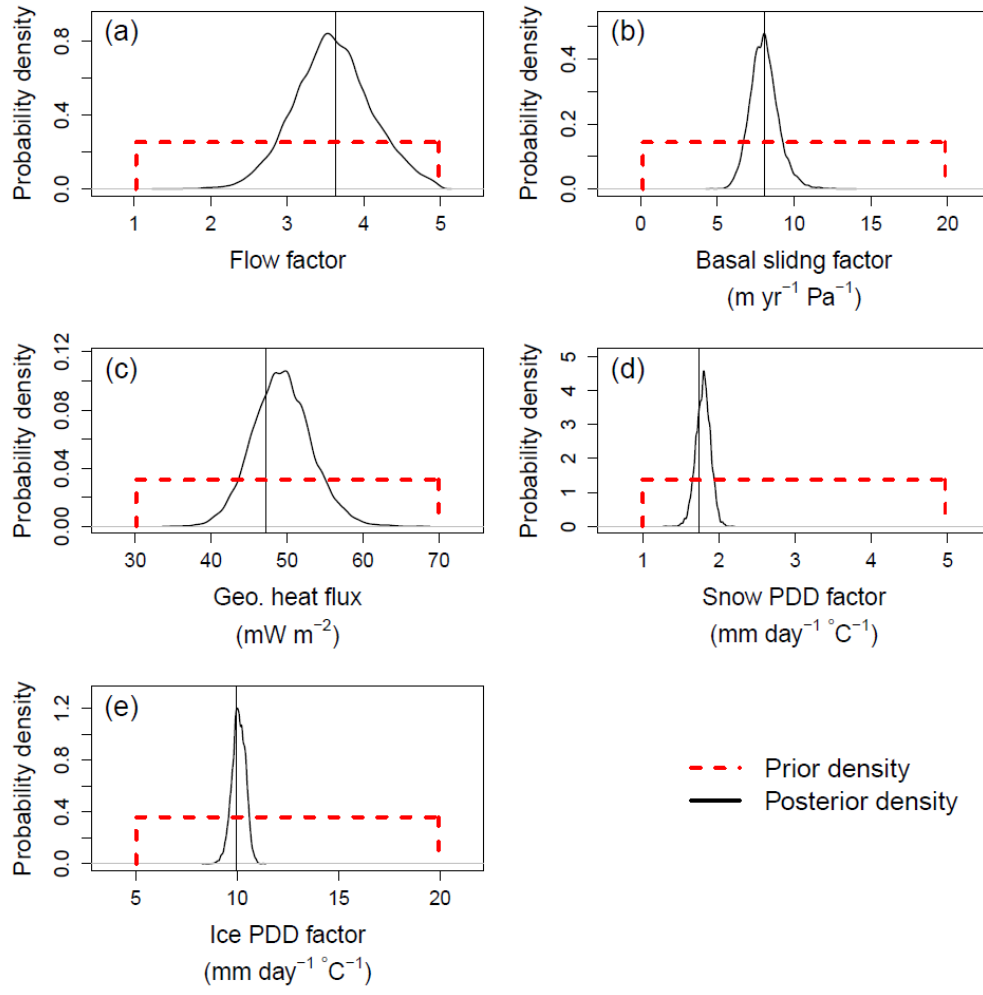
1
 2
 3 **Figure 1.** Profiles of zonal mean ice thicknesses from four different evaluations of the ice sheet
 4 model SICOPOLIS (Greve, 1997; Greve et al., 2011). The solid black curve represents model
 5 run #67 from Applegate et al. (2012), which we take to be the synthetic truth for our perfect
 6 model experiments. The other curves represent examples of model runs used to construct the
 7 emulator: one run produces a zonal mean ice thickness curve similar to the synthetic
 8 observations (dashed red curve), another is generally too thick (dotted green curve), and a third
 9 is generally too thin (dot-dashed blue curve). As expected, our probability model assigns a
 10 greater posterior probability to the model run represented by the red curve than to the model
 11 runs represented by the blue and green curves. All the other model runs that are not highlighted
 12 above are represented as grey curves.

13
 14



1
2

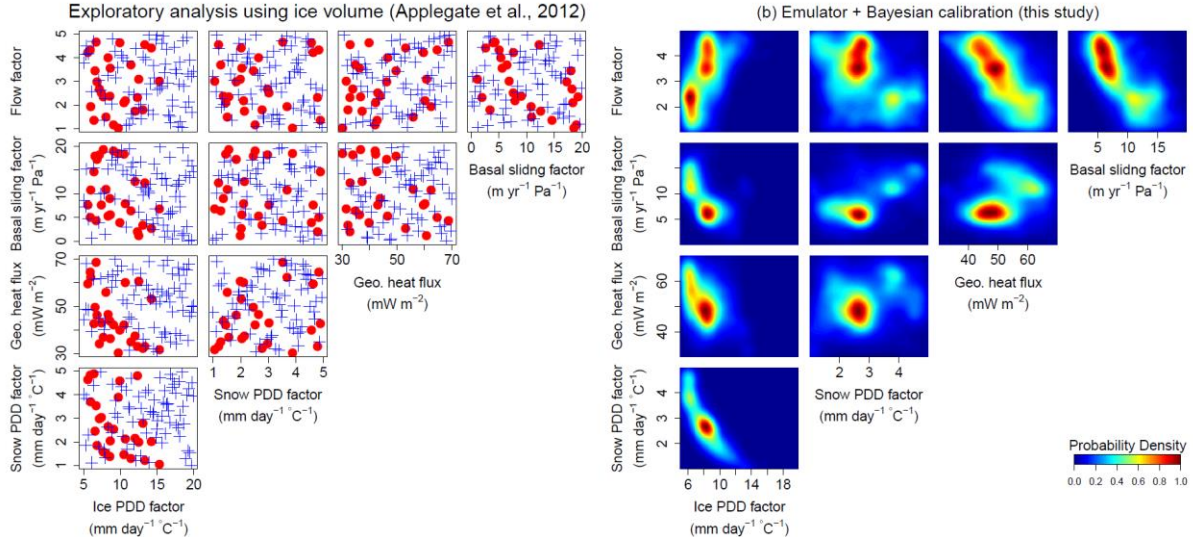
3 **Figure 2.** Comparison of zonal mean ice thickness transects from the assumed-true model run
4 (#67 from Applegate et al., 2012) and that generated by the trained emulator at the same
5 parameter combination as used in the assumed-true model run. In the top panel, the assumed-
6 true profile is shown by a solid black line, and the emulator output is shown by a dashed red
7 curve with circles. In the lower panel, each point stands for an individual latitude location. The
8 red circles in the top panel fall almost exactly on top of the black curve, and the points in the
9 lower panel fall almost exactly on a 1:1 line connecting the lower left and upper right corners
10 of the plot. Thus, the emulator successfully recovers the ice thicknesses from an assumed-true
11 model realization when trained on the other model runs from the same ensemble.



1

2

3 **Figure 3.** Prior (dashed red curves) and posterior (solid black curves) probability density
4 functions of each input parameter, assuming that all the other parameters are held fixed at their
5 assumed-true values. The vertical lines indicate the assumed-true values of the individual
6 parameters.



1
2
3
4
5
6
7
8
9
10
11
12

Figure 4. Comparison between an exploratory data analysis, following Applegate et al. (2012), and the results of our probabilistic calibration. (a) Scatterplots of parameter settings used to train the emulator, as projected onto two-dimensional marginal spaces. Red dots, parameter settings resulting in simulated modern ice volumes within 10% of the synthetic truth (model run #67 of Applegate et al. 2012); blue crosses, parameter settings that yield ice volumes more than 10% larger or smaller than the synthetic truth. (b) Two-dimensional marginal posterior densities of all pairs of input parameters. Several of the marginal posterior density maps show inclined bands of higher probability, indicating interactions among parameters; other panels show multiple modes, representing potential "traps" for tuning of ice sheet models using simpler methods. See text for discussion.

Illustrative projections based on synthetic data

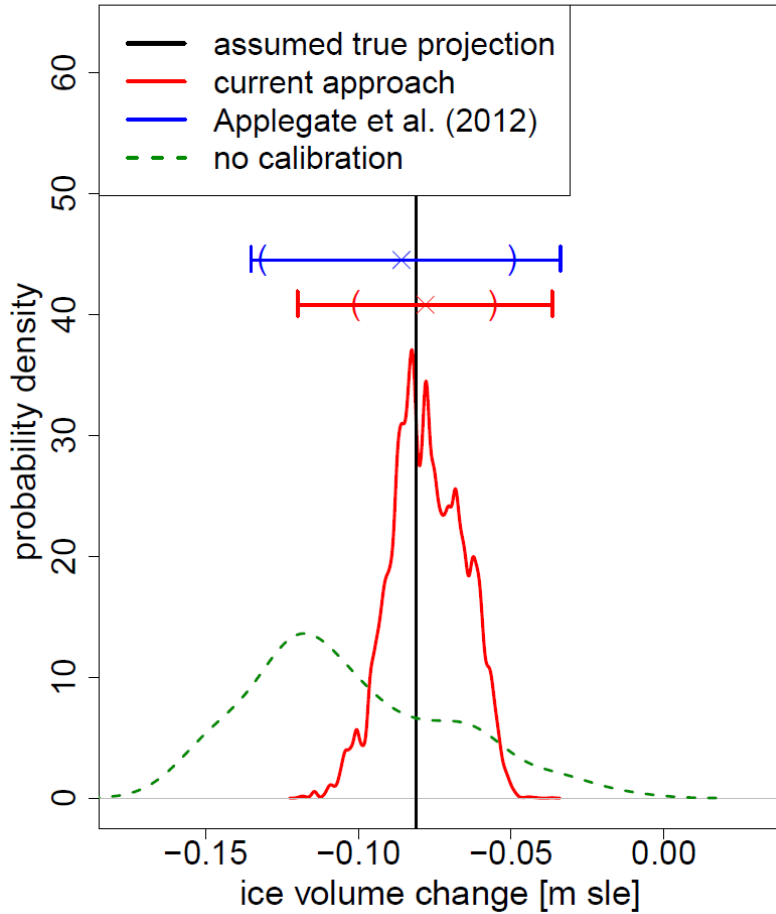


Figure 5. Illustrative (not "real") ice volume change projections between 2005 and 2100, based on three different methods: i) the prior density of the input parameters (dashed green line); ii) parameter settings that pass the 10% ice volume filter used by Applegate et al. (2012) (solid blue line); and iii) the posterior density computed by our calibration approach (solid red line). The vertical line shows the ice volume change projection for the assumed-true parameter setting. The horizontal lines and the parentheses on them represent the range and the 95% prediction intervals, respectively; the crosses indicate the median projection from each method. The width of the 95% projection interval from our methods is narrower than if simpler methods are applied (blue boxplot; Applegate et al., 2012). Similar results are obtained if different model runs from the ensemble are left out (see Figs. S3 and S4). See text for discussion. m sle, meters of sea level equivalent.

14